Central IL-1 receptor signaling regulates bone growth and mass

Alon Bajayo*†, Inbal Goshen†‡, Sharon Feldman*§, Valer Csernus¶, Kerstin Iverfeldt‖, Esther Shohami§, Raz Yirmiya‡, and Itai Bab*,**

*Bone Laboratory and Departments of ‡Psychology and §Pharmacology, Hebrew University of Jerusalem, Jerusalem 91120, Israel; ¶Department of Anatomy, University of Pécs Medical School and Neurohumoral Regulations Research Group of the Hungarian Academy of Sciences, H-7624 Pécs, Hungary; and ‖Department of Neurochemistry and Neurotoxicology, Stockholm University, 10691 Stockholm, Sweden

Edited by Charles A. Dinarello, University of Colorado Health Sciences Center, Denver, CO, and approved July 22, 2005 (received for review March 30, 2005)

The proinflammatory cytokine IL-1, acting via the hypothalamic IL-1 receptor type 1 (IL-1RI), activates pathways known to suppress bone formation such as the hypothalamo pituitary-adrenocortical axis and the sympathetic nervous system. In addition, peripheral IL-1 has been implicated as a mediator of the bone loss induced by sex hormone depletion and TNF. Here, we report an unexpected low bone mass (LBM) phenotype, including impairment of bone growth, in IL-1RI-deficient mice (IL-1rKO mice). Targeted overexpression of human IL-1 receptor antagonist to the central nervous system using the murine glial fibrillary acidic protein promoter (IL-1raTG mice) resulted in a similar phenotype, implying that central IL-1RI silencing is the causative process in the LBM induction. Analysis of bone remodeling indicates that the process leading to the LBM in both IL-1rKO and IL-1raTG is characterized mainly by doubling the osteoclast number. Either genetic modification does not decrease testosterone or increase corticosterone serum levels, suggesting that systems other than the gonads and hypothalamo pituitary-adrenocortical axis mediate the central IL-1RI effect on bone. We further demonstrate that WT mice express mouse IL-1ra in bone but not in the hypothalamus. Because low levels of IL-1 are present in both tissues, it is suggested that skeletal IL-1 activity is normally suppressed, whereas central IL-1 produces a constant physiologic stimulation of IL-1RI signaling. Although the pathway connecting the central IL-1RI signaling to bone remodeling remains unknown, the outburst of osteoclastogenesis in its absence suggests that normally it controls bone growth and mass by tonically restraining bone resorption.

bone remodeling | bone resorption | brain | central regulation | IL-1 receptor antagonist

IL-1 is a proinflammatory cytokine produced by many types of cells, including peripheral immune and bone cells, as well as glia and neuron cells in the CNS (1, 2). The soluble ligands IL-1α and IL-1β are believed to exert identical actions by binding to a single cell surface receptor (IL-1RI) (3), which also requires the association with an accessory protein (AcP) for its activation (4). A second receptor (IL-1RII) also binds IL-1, but lacks an intracellular domain and does not initiate signal transduction (5). IL-1 signaling is restrained by the IL-1 receptor antagonist (IL-1ra), a highly selective, endogenous competitive IL-1 inhibitor. IL-1ra is expressed in a multitude of tissues (6), binds to IL-1RI, but fails to trigger the association between IL-1RI and AcP, which is essential for subsequent signaling (4). In addition to the endogenous inhibition of IL-1 activity, IL-1ra is a valuable experimental tool to study the pathophysiologic role of IL-1RI signaling.

In vertebrates, bone mass and shape are determined by continuous remodeling consisting of the concerted action of osteoclasts, the bone-resorbing cells, and osteoblasts, the bone-forming cells. IL-1 is an important proresorptive cytokine (1, 7); although alone it does not induce osteoclastogenesis, it potently stimulates osteoclast differentiation induced by colony stimulating factor and receptor activator of NF-κB (8). Peripheral IL-1ra administration decreases osteoclast formation and bone resorption in ovariectomized mice (9), and IL-1RI-deficient mice do not lose bone after ovariectomy (10), implying an important role for IL-1 in the bone loss induced by gonadal hormone depletion. IL-1 is also a key mediator of TNF-induced bone resorption (11).

IL-1 and IL-1RI are expressed by brain cells, although at low levels in the healthy CNS (12). In health, the central IL-1 system has been implicated in modulating sleep patterns (13) as well as in learning and memory (14). Using IL-1RI-deficient mice and mice with CNS-targeted IL-1ra overexpression, we show here that central IL-1 receptor signaling is also a potent regulator of bone growth, bone remodeling, and bone mass.

Materials and Methods

Animals. Male 5- and 15-week-old mice were used throughout the study. Mice deficient of IL-1RI (IL-1rKO) and their 129/Sv $\times$ C57BL/6 WT controls (15) were obtained from The Jackson Laboratory. Mice with homozygous transgenic overexpression of the secreted human IL-1ra in astrocytes within the CNS (IL-1raTG) were generated on a C57BL/6 $\times$ CBA background. They were first developed as a heterozygous strain (16). The homozygous line was then established by crossing the heterozygous mice (17). These mice were generated in the Department of Neurochemistry and Neurotoxiocology, Stockholm University, and Neurotec Department, Karolinska University Hospital (Huddinge, Sweden). Both the IL-1rKO and homozygous IL-1raTG mice lack central responses to exogenously administered or endogenous IL-1 (15, 17–19). No differences in vitality were found between these strains and their respective WT controls. Four days and 1 day before killing, the animals were given the fluorochrome calcein intraperitoneally (15 mg/kg) (Sigma). The calcein is incorporated into newly formed bone, and the extent of labeled trabecular surface and distance between the two labels are used to assess osteoblast activity by using fluorescent microscopy and dynamic histomorphometry (see below). The experiments were approved by the Hebrew University Committee of Animal Care and Use.

Microcomputed Tomographic (μCT) Analysis. Whole femora (one per mouse) and bodies of the third lumbar vertebra (L3) were examined by a μCT system (Desktop μCT 40, Scanco Medical AG, Bassersdorf, Switzerland). The scans were performed at a

This paper was submitted directly (Track II) to the PNAS office.

Abbreviations: IL-1RI, IL-1 receptor type 1; IL-1ra, IL-1 receptor antagonist; hIL-1ra, human IL-1ra; IL-1rKO, IL-1RI-deficient mice; μCT, microcomputed tomography; BV/TV, bone volume density; Tb.Th, trabecular thickness; Tb.N, trabecular number; Conn.D, trabecular connectivity density; TRAP, tartrate-resistant acid phosphatase; MAR, mineral appositional rate; Min.Peri, mineralizing perimeter; BFR, bone formation rate; LBM, low bone mass; IL-1raTG, transgenic mice with CNS expression of hIL-1ra.

†A.B. and I.G. contributed equally to this work.

**To whom correspondence should be addressed at: Hebrew University of Jerusalem, Institute of Dental Sciences, Bone Laboratory, Jerusalem 91120, Israel. E-mail: babi@cc.huji.ac.il.

© 2005 by The National Academy of Sciences of the USA

20-μm resolution in all three spatial dimensions. 2D CT images were reconstructed in 512 $\times$ 512 pixel matrices by using a standard convolution-back projection procedure with a Shepp and Logan filter. Images were stored in 3D arrays with an isotropic voxel size of 20 μm. A constrained 3D Gaussian filter was used to partly suppress the noise in the volumes. The mineralized tissues were differentially segmented by a global thresholding procedure (20). All morphometric parameters were determined by using a direct 3D approach (21). In femora, we analyzed three preselected regions: (*i*) whole bone (including articular ends); (*ii*) secondary spongiosa in the distal metaphysis extending proximally 3 mm from the proximal tip of the primary spongiosa; and (*iii*) a diaphyseal segment extending 1 mm distally from the midpoint between the femoral ends. For the whole bone, we determined the external dimensions. Parameters determined in the metaphyseal trabecular bone included bone volume density (BV/TV), trabecular thickness (Tb.Th), trabecular number (Tb.N) and trabecular connectivity density (Conn.D). Cortical thickness (Cort.Th), total diaphyseal diameter (Dia.Dia), and the medullary cavity diameter (Med.Dia) were determined in the mid-diaphyseal region. In L3 bodies, we analyzed the entire trabecular bone compartment.

Histomorphometry. After μCT image acquisition, the same femora were dehydrated in progressive concentrations of ethanol, cleared in xylene, and embedded undecalcified in polymethylmethacrylate (Technovit 9100, Heraeus Kulzer). Undeplasticized, longitudinal 5-μm sections were left unstained for dynamic histomorphometric measurements. To identify osteoclasts, consecutive sections were deplasticized and stained for tartrate-resistant acid phosphatase (TRAP) by using an acid phosphatase kit (Sigma) and counterstained with Mayer's hematoxylin. TRAP staining is specific to osteoclasts (22). Histomorphometric analysis was carried out on digital photomicrographic images by using IMAGE-PRO EXPRESS 4.0.1V image analysis software (Media Cybernetics, Silver Spring, MD). The following parameters were determined: mineral appositional rate (MAR), mineralizing perimeter (Min.Peri), bone formation rate (BFR), and osteoclast number (N.Oc/BS). Cross sections through the mid-diaphyseal region were used to measure endosteal and periosteal MAR. The terminology and units used for these measurements were according to the convention of standardized nomenclature (23).

hIL-1ra ELISA. Expression of hIL-1ra protein in the cerebral cortex and blood was analyzed by ELISA (R & D Systems).

mRNA Analysis. Total RNA was extracted from the freshly isolated hypothalami and trabecular bone sites (distal femoral and proximal tibial metaphyses), purified, and reverse transcribed by using routine procedures. The following primers were used for PCR: mouse IL-1ra (mIL-1ra), sense, 5′-GAC CCT GCA AGA TGC AAG CC-3′, antisense, 5′-CAG GAC GGT CAG CCT CTA GT-3′; human soluble IL-1ra (hIL-1ra), sense, 5′-CGA CCC TCT GGG AGA AAA TC-3′, antisense, 5′-CTC ATC ACC AGA CTT GAC AC-3′; and β-actin, sense, 5′-GAG ACC TTC AAC ACC CCA GCC-3′, antisense, 5′-GGC CAT CTC TTG CTC GAA GTC-3′. PCR conditions were as reported (16).

Serum Corticosterone and Testosterone Measurements. Collection of blood samples and radioimmunoassays were carried out as described (24, 25). The sensitivity limit of the corticosterone assay was 0.5 μg/100 ml, and the intra- and interassay coefficients of variation (CV) were 6.4% and 7.2%, respectively. The percentage of crossreactivity of the antiserum with various steroids was as follows: cortisol, 4.5%; estradiol, <0.1%; progesterone, 15.7%; and testosterone, 7.9%. The sensitivity limit of the testosterone assay was 3 fmol per tube. The interassay and intraassay CV were 9.8% and 5.9%, respectively.

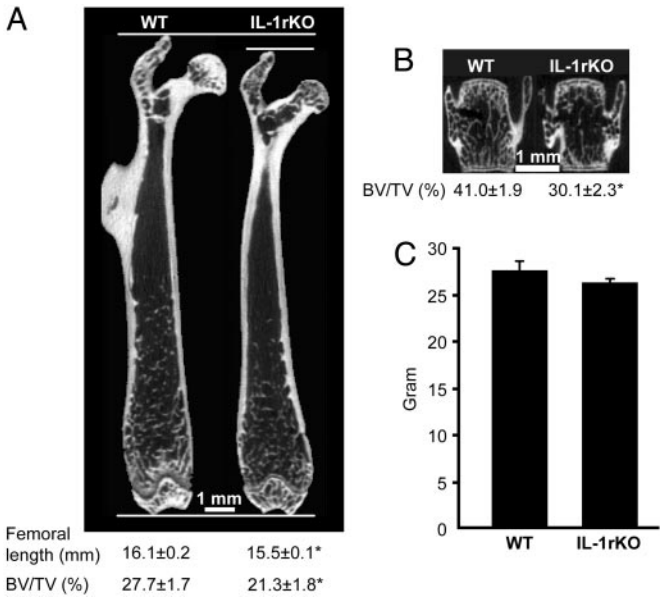

Fig. 1. Skeletal growth impairment and low bone mass phenotype in IL-1rKO mice. (*A* and *B*) Qualitative (2D images) and quantitative μCT analysis showing reduction in femoral length and decreased trabecular bone volume density (BV/TV, volume of trabecular network as percentage of total reference volume) in distal femoral metaphysis (*A*) and L3 vertebra (*B*). (*C*) Body weight. Data are mean $\pm$ SE obtained in 10 animals per condition. *, *t* test; $P < 0.05$.

Results

Low Bone Mass (LBM) Phenotype in IL-1rKO Mice. A previous histomorphometric study (10) in the proximal humerus reported a normal bone mass in IL-1rKO mice of the same line. Although at low levels, IL-1 is present in the serum of healthy animals (26), which made us wonder whether a more comprehensive analysis of the IL-1rKO phenotype would exhibit a high bone mass phenotype that can be expected from the absence of IL-1 receptor signaling. Unexpectedly, the μCT analysis, which takes into account the entire volume of the trabecular bone compartment, clearly demonstrated a moderately LBM phenotype in both the distal femoral metaphysis and L3 vertebral bodies (Fig. 1 *A* and *B*). By comparison with the WT controls, the respective BV/TV values in the IL-1rKO mice were 23% and 27% lower in the femora and vertebrae. The LBM was associated with decreased Tb.Th and Tb.N, which reached statistical significance in the femora and vertebrae, respectively (Table 1). The μCT analysis also demonstrated impairment of skeletal growth in these mice, reflected by 0.6 mm shorter femora compared with the controls (Fig. 1*A*). These changes could not be explained by reduced physical activity or food intake, because the IL-1rKO are fully active (data not shown) and of normal weight (Fig. 1*C*).

LBM Phenotype in IL-1raTG Mice. Unlike the proinflammatory action of peripheral IL-1 receptor signaling, activation of the central IL-1RI restrains the peripheral immune system (27–29). Hence, because the osteoclast is a hematopoietic cell that branches from the monocyte-macrophage lineage (30), we assumed that the LBM phenotype and impaired bone growth in the IL-1rKO mice result from the absence of central IL-1RI signaling and a consequent increase in bone resorption. To address this issue, we characterized the osteogenic phenotype of mice with transgenic overexpression of hIL-1ra targeted to the CNS by using the glial fibrillary acidic protein (GFAP) promoter. It has

Table 1. Morphometric μCT parameters in trabecular bone of IL-1rKO mice

	Femur			L3		
Mouse	Tb.N, 1/mm	Tb.Th, μm	Conn.D, 1/mm³	Tb.N, 1/mm	Tb.Th, μm	Conn.D, 1/mm³
IL-1rKO	4.99 ± 0.09	76 ± 4*	60.6 ± 4.5	4.69 ± 0.09*	79 ± 2	89.7 ± 5.3
WT†	5.21 ± 0.21	91 ± 3	68.0 ± 8.4	5.93 ± 0.06	83 ± 2	97.9 ± 4.5

Data are mean ± SE obtained in 10 mice per condition. *, *t* test; $P < 0.05$.
†WT controls were 129/Sv × C57BL/6 mice.

been previously demonstrated that the cerebral hIL-1ra level in the present homozygous IL-1raTG mouse line is >200-fold higher than in WT controls (17). Our confirmatory measurements in the cerebral cortex of IL-1raTG and WT mice were 413 ± 35 pg/mg tissue (mean ± SE) and nondetectable (<0.1 pg/mg tissue), respectively. In addition, no hIL-1ra levels were detected in the serum of either IL-1raTG or WT mice. It was previously reported that hIL-1ra is nondetectable in peripheral tissues of the parent heterozygous mice, such as the liver, spleen, and skeletal muscle (16). To rule out possible skeletal expression of the transgene and consequent effect on bone metabolism, we have analyzed IL-1ra mRNA levels comparatively in the hypothalamus and trabecular bone (which contains a significant amount of bone marrow). In WT animals, hIL-1ra mRNA was not detected in bone or the hypothalamus (Fig. 2*A*). By contrast, the hIL-1ra transgene was strongly expressed in the hypothalamus of the IL-1raTG mice but not in bone (Fig. 2*B*). As previously reported (9, 16), in both mouse lines the expression of mouse IL-1ra (mIL-1ra) was substantial in bone but nondetectable in the hypothalamus (Fig. 2). It should be pointed out that, in the reported studies or herein, there was no attempt to separate components of the peripheral nervous system from the tissue samples that were analyzed. Therefore, although the GFAP promoter may potentially drive expression in Schwann and other peripheral cells (31), no evidence was obtained for the presence of the hIL-1ra mRNA or protein other than in the brain.

Despite a different genetic background than the IL-1rKO, the IL-1raTG mice showed a similar, although more pronounced LBM. The femora of both young and adult IL-1raTG mice were shorter by almost 1 mm compared with the WT animals (Fig. 3*A*). In addition, their mean diaphyseal diameter was smaller by >100 μm (Fig. 3*B*). Likewise, by comparison with the WT mice, the medullary cavity diameter of the IL-1raTG animals was significantly smaller (Fig. 3*B*). These differences could not be ascribed to reduced body mass, because the young IL-1raTG and WT animals were of the same weight and the adult IL-1raTG mice were even heavier than the controls (Fig. 3*C*).

Because the regulation of trabecular bone mass may differ among skeletal sites (32), we analyzed the cancellous compartment in the distal femoral metaphysis and L3 bodies. In the young and adult IL-1raTG mice, both sites showed a LBM (Fig. 4*A*). In the young transgenic animals, the respective BV/TV values in L3 bodies and the distal femur were 25% and 29% lower than in the WT controls. In the adult IL-1raTG mice, this difference increased to 37% and 49% in the L3 bodies and distal femur, respectively (Fig. 4 *B* and *C*). In the adult mice, the qualitative and quantitative analyses in these sites showed that the reduced BV/TV was accompanied by lower than control

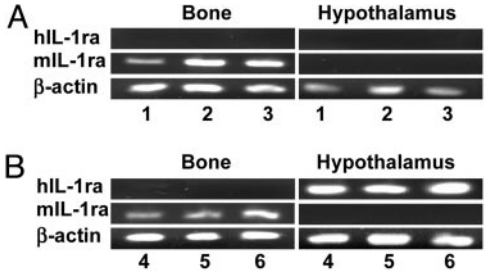

Fig. 2. Central and skeletal expression of IL-1ra. RT-PCR analysis using primers for human (hIL-1ra) and mouse (mIL-1ra) cDNA. (*A*) WT mice; similar results were obtained in six animals. (*B*) IL-1raTG mice; similar results were obtained in six animals. Numbers indicate representative animals used for mRNA extraction.

Fig. 3. Central IL-1RI signaling regulates longitudinal and radial bone growth. (*A* and *B*) Qualitative (3D) and quantitative μCT analysis showing reduction in femoral length (*A*), in diaphyseal diameter (Dia.Dia) and medullary cavity diameter (Med.Dia) (*B*) in IL-1raTG mice. Shown are images obtained from mice with median length (*A*) and diaphyseal diameter (*B*). Dashed lines in *A* indicate position of diaphyseal segments shown in *B*. (*C*) Body weight in 5-week-old (*Upper*) and 15-week-old (*Lower*) mice. Data are mean ± SE in five 5-week-old and twelve 15-week-old mice per condition. *, *t* test; $P < 0.05$.

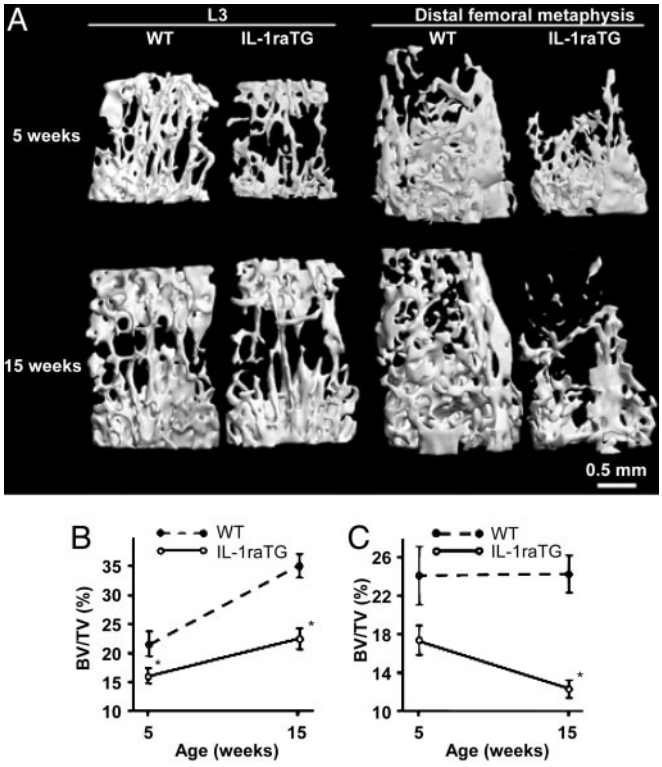

Fig. 4. Low trabecular bone mass phenotype in IL-1raTG mice. (*A*) Qualitative (3D) μCT analysis. (*B* and *C*) μCT analysis of trabecular bone volume density (BV/TV, volume of trabecular network as percentage of total reference volume) in L3 vertebra (*B*) and distal femoral metaphysis (*C*). Data are mean ± SE in five 5-week-old and twelve 15-week-old mice per condition. *, *t* test; $P <$ 0.05.

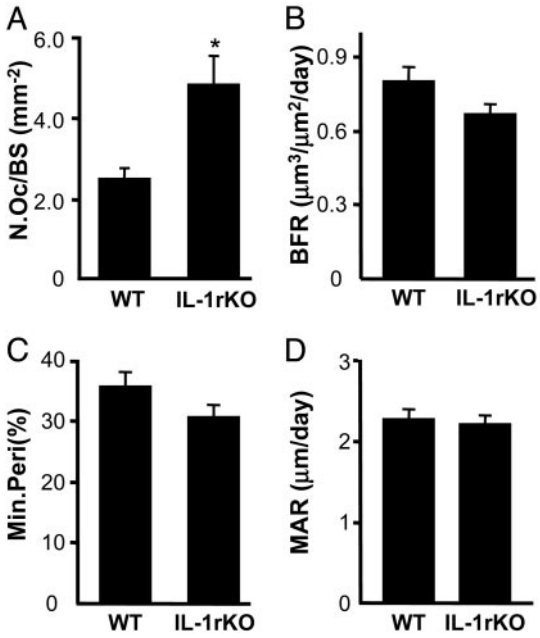

Fig. 5. Elevated osteoclast number in IL-1rKO mice. Shown is a histomorphometric analysis. (*A*) Osteoclast number, surrogate of bone resorption activity, calculated as the number of TRAP-positive osteoclasts per trabecular surface area. (*B–D*) Measurements based on fluorescent calcein labeling of newly formed bone. (*B*) BFR, surrogate of total bone formation activity, calculated as the arithmetic product of MAR and Min.Peri. (*C*) Min.Peri, surrogate of osteoblast number, calculated as the percentage of calcein-labeled trabecular surface. (*D*) MAR, surrogate of osteoblast activity, calculated as the average distance between two calcein-labeled lines divided by the time interval between the two calcein injections. Data are mean ± SE in nine animals per condition. *, *t* test; $P < 0.05$.

Tb.N and Tb.Th (Fig. 4*A* and Table 2). Conn.D, which reflects the level of structural integrity of the trabecular network, was also lower in the IL-1raTG than WT animals. Although the same trend was noticed in the 5-week-old transgenic mice, the differences at this age were smaller than in the adult animals and did not reach statistical significance (Table 2). Jointly, these data suggest that silencing of the central IL-1RI signaling leads to a progressing impairment in the accrual and perhaps maintenance of bone mass.

Increased Bone Resorption in IL-1rKO and IL-1raTG Mice. LBM inevitably results from a negatively balanced bone remodeling with a net increase in bone resorption (33). To investigate changes in bone remodeling, we measured trabecular bone resorption and formation parameters in the femoral metaphysis of IL-1rKO and adult IL-1raTG mice and their respective 129/Sv × C57BL/6 and C57BL/6 × CBA WT controls. As for the other μCT and histomorphometric parameters, the osteoclast number (N.Oc/BS) did not differ significantly between the two WT mouse lines (Figs. 5 and 6). In addition, in both engineered mouse lines it was ≈2-fold higher compared with the respective WT animals (Figs. 5*A* and 6*A*). Whereas in the IL-1rKO bone formation remained unchanged (Fig. 5 *B–D*), the IL-1raTG mice showed increased BFR (Fig. 6*B*) secondary to increases in both the Min.Peri (Fig. 6*C*) and MAR (Fig. 6*D*). The increase in BFR was substantially less than the increase in N.Oc/BS. These data indicate a striking increase in bone resorption, which in the IL-1raTG mice was accompanied by a moderate increase in bone formation, as observed in many osteoporotic states in humans and experimental animals.

Pathways Other than the Hypothalamic-Pituitary-Adrenal (HPA)-, and Hypothalamic-Pituitary-Gonadal (HPG) Axes Communicate the Central IL-1 Signal to Bone. Gonadal hormones and glucocorticoids are among the most powerful regulators of bone remodeling (34, 35). To assess their possible involvement in mediating the effects of defective IL-1RI signaling on bone and the development of

Table 2. Morphometric μCT parameters in trabecular bone of IL-1raTG mice

		Femur			L3		
Mouse	Age, wk	Tb.N, 1/mm	Tb.Th, μm	Conn.D, 1/mm^3	Tb.N, 1/mm	Tb.Th, μm	Conn.D, 1/mm^3
IL-1raTG	5	3.79 ± 0.13	78 ± 4	53.9 ± 2.8	4.35 ± 0.19	64 ± 1	72.4 ± 12.8
WT†		4.45 ± 0.34	88 ± 5	56.7 ± 4.4	4.80 ± 0.16	69 ± 5	98.0 ± 8.2
IL-1raTG	15	2.32 ± 0.16*	97 ± 2*	14.3 ± 1.3*	3.55 ± 0.17*	81 ± 3*	50.4 ± 4.4*
WT†		3.74 ± 0.28	104 ± 2	35.5 ± 4.6	4.90 ± 0.14	88 ± 2	75.7 ± 3.3

Data are mean ± SE in five 5-week-old and twelve 15-week-old mice per condition. *, *t* test; $P < 0.05$.
†WT controls were C57BL/6 × CBA mice.

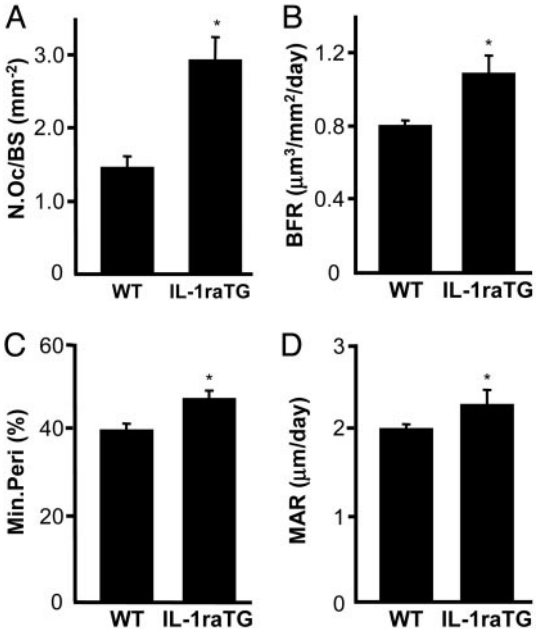

Fig. 6. High trabecular bone turnover in IL-1raTG mice. Shown is a histomorphometric analysis in 15-week-old mice. (*A*) Osteoclast number, surrogate of bone resorption activity, calculated as the number of TRAP-positive osteoclasts per trabecular surface area. (*B–D*) Measurements based on fluorescent calcein labeling of newly formed bone. (*B*) BFR, surrogate of total bone formation activity, calculated as the arithmetic product of MAR and Min.Peri. (*C*) Min.Peri, surrogate of osteoblast number, calculated as the percent calcein-labeled trabecular surface. (*D*) MAR, surrogate of osteoblast activity, calculated as the average distance between two calcein-labeled lines divided by the time interval between the two calcein injections. Data are mean ± SE in five to six animals per condition. *, *t* test; $P < 0.05$.

LBM in the IL-1rKO and IL-1raTG mice, we measured the serum levels of corticosterone and testosterone. The corticosterone levels were the same in the engineered and WT mice (Table 3). The serum testosterone was similar in the IL-1rKO mice and their 129/Sv × C57BL/6 WT controls. In the IL-1raTG animals, they were higher than in the normal C57BL/6 × CBA mice (Table 3). Jointly, these measurements suggest that pathways other than the HPA and HPG axes communicate the effect of central IL-1RI signaling on bone remodeling.

Discussion

Studying mice with generalized and CNS-targeted silencing of IL-RI signaling, we uncover here involvement of a central system in the physiologic regulation of bone growth and mass. The key role of the central IL-1 system in bone remodeling is demonstrated by the magnitude of the LBM in both the IL-1rKO and IL-1raTG mice. Furthermore, the effect of central IL-1RI silencing on bone is independent of the mouse strain used inasmuch as the IL-1rKO and IL-1raTG lines have different genetic backgrounds.

Table 3. Serum levels of bone mass-regulating steroid hormones in IL-1rKO and IL-1raTG mice

Mouse	Corticosterone, μg/dl	Testosterone pmol/liter
IL-1rKO[†]	1.33 ± 0.24	2,546 ± 376
WT[†‡]	1.11 ± 0.18	2,645 ± 414
IL-1raTG	0.95 ± 0.07	2,583 ± 15*
WT[§]	0.94 ± 0.09	1,568 ± 31

Data are mean ± SE obtained in 12 mice per condition. *, *t* test; $P < 0.05$.
[†]Ref. 18.
[‡]Background mouse strain for the IL-1rKO mice was 129/Sv × C57BL/6.
[§]Background mouse strain for the IL-1raTG mice was C57BL/6 × CBA.

In humans, bone mass is determined by two supposedly independent processes: accrual of peak bone mass and age-dependent bone loss (36). In mice, where skeletal growth, including enchondral elongation, continues long after sexual maturation (37), these processes cannot be completely separated from each other. Still, the present impairment of bone growth resulting from the absence of central IL-1RI signaling on the one hand and the progressive inhibition in trabecular bone density in maturing animals on the other suggest that inactivation of central IL-1RI inhibits peak bone mass accrual during the active phase of skeletal development and attenuates its maintenance in older age.

When administered to normal mice, IL-1 enhances bone resorption and causes hypercalcemia (38, 39) by increasing the pool size of preosteoclasts in bone marrow (40, 41). In addition, IL-1 is a potent stimulator of the differentiation, activation, and survival of osteoclasts (42). It was recently demonstrated that ligation of IL-1RI results in hyperactivation of NF-κB and mitogen-activated protein (MAP) kinase signaling pathways, which are essential for osteoclast differentiation (43). IL-1 stimulation of NF-κB is a key processes in osteoclastic bone destruction in rheumatoid arthritis (44). Therefore, it is surprising that the skeletal effect of central IL-1RI silencing, namely, the net increase in osteoclast number and activity, is similar to the effect of IL-1RI signaling in bone and contrasts the skeletal effects of peripherally administered IL-1ra (9, 11). The osteoclastogenic effect of central IL-1RI silencing cannot be ascribed to a compensatory increase in IL-1RI agonists, because (*i*) they are not effective in the IL-1rKO mice where IL-1RI is blocked irreversibly; and (*ii*) although IL-1ra inhibition of IL-1RI signaling is of a reversible nature, the IL-1raTG mice lack central responses to exogenously administered or elevated endogenous IL-1β (15, 17–19), probably because of the vast excess of the transgenic protein. Despite the marked increase in osteoclastogenesis in both the IL-1rKO and IL-1raTG mice, the effect of either genetic manipulation is not mediated through gonadal hormone deficiency, known for its fundamental effects on bone remodeling (34). Likewise, glucocorticoids, also known for their negative regulation of bone mass (45), remain uninvolved in the LBM induced by the absence of central IL-1RI signaling.

Although at low levels, IL-1 is normally expressed in bone and in the hypothalamus and other parts of the CNS (11, 46, 47). Our demonstration of WT IL-1ra expression in bone may suggest that most, if not all, of the skeletal IL-1 activity is normally suppressed. By contrast, the absence of detectable hypothalamic IL-1ra expression in WT mice implies constant, physiologic central IL-1RI signaling. This conclusion is further supported by the phenotypic similarities between the IL-1raTG and IL-1rKO mice. Although the pathway connecting the central IL-1RI signaling to bone remodeling remains unknown, the outburst of osteoclastogenesis in its absence suggests that normally it controls bone growth and mass by tonically restraining bone resorption.

In vertebrates, bone mass is maintained constant through the opposing but balanced action of osteoblasts and osteoclasts (35). It has been suggested that this balance results from the coupling between bone resorption and bone formation understood as an osteoblastic response evoked by osteoclastic activity, with an amount of bone formed that is equal to that resorbed (48, 49). With the previous discovery of a physiologic brain-to-bone pathway in the regulation of osteoblast activity (50, 51) and the present demonstration of a central system controlling osteoclastogenesis, it is tempting to speculate that the CNS is involved in

the coupling process in bone in unusual ways that require further investigation.

We thank J. Weidenfeld for his contribution to the serum corticosterone analysis and O. Lahat for technical assistance. E.S. is affiliated with the David R. Bloom Center for Pharmacy, Hebrew University School of Pharmacy, Jerusalem. This work was supported by Israel Science Foundation (ISF) Grant 4007/02-Bikura (to I.B., R.Y., and E.S.). Purchase of the μCT system was supported in part by ISF Grant 9007/01 (to I.B.).

1. Lorenzo, J. A., Sousa, S. L., Van den Brink-Webb, S. E. & Korn, J. H. (1990) *J. Bone Miner. Res.* **5,** 77–83.
2. Dinarello, C. A. (1997) *Cytokine Growth Factor Rev.* **8,** 253–265.
3. Sims, J. E., March, C. J., Cosman, D., Widmer, M. B., MacDonald, H. R., McMahan, C. J., Grubin, C. E., Wignall, J. M., Jackson, J. L., Call, S. M., *et al.* (1988) *Science* **241,** 585–589.
4. Scott, A., Greenfeder, S. A., Nunes, P., Kwee, L., Labow, M., Chizzonite, R. A. & Ju, G. (1995) *J. Biol. Chem.* **27,** 13757–13765.
5. Sims, J. E., Gayle, M. A., Slack, J. L., Alderson, M. R., Bird, T. A., Giri, J. G., Colotta, F., Re, F., Mantovani, A., Shanebeck, K., *et al.* (1993) *Proc. Natl. Acad. Sci. USA* **90,** 6155–6159.
6. Arend, W. P., Malyak, M., Guthridge, C. J. & Gabay, C. (1998) *Annu. Rev. Immunol.* **16,** 27–55.
7. Dinarello, C. A. (1991) *Blood* **77,** 1627–1652.
8. Ma, T., Miyanishi, K., Suen, A., Epstein, N. J., Tomita, T., Smith, R. L. & Goodman, S. B. (2004) *Cytokine* **26,** 138–144.
9. Kitazawa, R., Kimble, R. B., Vannice, J. L., Kung, V. T. & Pacifici, R. (1994) *J. Clin. Invest.* **94,** 2397–2406.
10. Lorenzo, J. A., Naprta, A., Rao, Y., Alander, C., Glaccum, M., Widmer, M., Gronowicz, G., Kalinowski, J. & Pilbeam, C. C. (1998) *Endocrinology* **139,** 3022–3025.
11. Wei, S., Kitaura, H., Zhou, P., Ross, F. P. & Teitelbaum, S. L. (2005) *J. Clin. Invest.* **115,** 282–290.
12. Rothwell, N. J. & Luheshi, G. N. (2000) *Trends Neurosci.* **23,** 618–625.
13. Krueger, J. M., Fang, J., Taishi, P., Chen, Z., Kushikata, T. & Gardi, J. (1998) *Ann. N.Y. Acad. Sci.* **856,** 148–159.
14. Avital, A., Goshen, I., Kamsler, A., Segal, M., Iverfeldt, K., Richter-Levin, G. & Yirmiya, R. (2003) *Hippocampus* **13,** 826–834.
15. Labow, M., Shuster, D., Zetterstorm, M., Nunes, P., Terry, R., Cullinan, E. B., Bartfai, T., Solorzano, C., Moldawer, L. L., Chizzonite, R., *et al.* (1997) *J. Immunol.* **159,** 2452–2461.
16. Lundkvist, J., Sundgren-Andersson, A. K., Tingsborg, S., Östlund, P., Engfors, C., Alheim, K., Bartfai, T., Iverfeldt, K. & Schultzberg, M. (1999) *Am. J. Physiol.* **276,** 644–651.
17. Tehranian, R., Andell-Jonsson, S., Beni, S. M., Yatsiv, I., Shohami, E., Bartfai, T., Lundkvist, J. & Iverfeldt, K. (2002) *J. Neurotrauma* **19,** 939–951.
18. Goshen, I., Yirmiya, R., Iverfeldt, K. & Weidenfeld, J. (2003) *Endocrinology* **144,** 4453–4458.
19. Shavit, Y., Wolf, G., Goshen, I., Livshits, D. & Yirmiya, R. (2005) *Pain* **115,** 50–59.
20. Rüegsegger, P., Koller, B. & Müller, R. (1996) *Calcif. Tiss. Int.* **58,** 24–29.
21. Hildebrand, T., Laib, A., Müller, R., Dequeker, J. & Rüegsegger, P., (1999) *J. Bone Miner. Res.* **14,** 1167–1174.
22. Erlebacher, A. & Derynck, R. (1996) *J. Cell. Biol.* **132,** 195–210.
23. Parfitt, A. M., Drezner, M. K., Glorieux, F. H., Kanis, J. A., Malluche, H., Meunier, P. J., Ott S. M. & Recker, R. R. (1987) *J. Bone Miner. Res.* **2,** 595–610.
24. Weidenfeld, J. & Yirmiya, R. (1996) *Neuroimmunomodulation* **3,** 352–357.
25. Wenger, T., Ledent, C., Csernus, V. & Gerendai, I. (2001) *Biochem. Biophys. Res. Commun.* **284,** 363–368.
26. Schulze, P. C., Gielen, S., Adams, V., Linke, A., Möbius-Winkler, S., Erbs, S., Kratzsch, J., Hambrecht, R. & Schuler, G. (2003) *Basic Res. Cardiol.* **98,** 267–274.
27. Irwin, M. (1993) *Endocrinology* **133,** 1352–1360.
28. Sullivan, G. M., Canfield, S. M., Lederman, S., Xiao, E., Ferin, M. & Wardlaw, S. L. (1997) *Neuroimmunomodulation* **4,** 12–18.
29. Hodgson, D. M., Yirmiya, R., Chiappelli, F. & Taylor, A. N. (1999) *Brain Res.* **816,** 200–208.
30. Roodman, G. D. (1999) *Exp. Hematol.* **27,** 1229–1241.
31. Su, M., Hu, H., Lee, Y., d'Azzo, A., Messing, A. & Brenner, M. (2004) *Neurochem. Res.* **29,** 2075–2093.
32. Sheng, M. H., Baylink, D. J., Beamer, W. G., Donahue, L. R., Lau, K. H. & Wergedal, J. E. (2002) *Bone* **30,** 486–491.
33. Mishina, Y., Starbuck, M. W., Gentile, M. A., Fukuda, T., Kasparcova, V., Seedor, J. G., Hanks, M. C., Amling, M., Pinero, G. J., Harada, S., *et al.* (2004) *J. Biol. Chem.* **279,** 27560–27566.
34. Balasch, J. (2003) *Hum. Reprod. Update* **9,** 207–222.
35. Manolagas, S. C. (1998) *Aging* **10,** 182–190.
36. Seeman, E. (2003) *Endocrinol. Metab. Clin. North Am.* **32,** 25–38.
37. Kilborn, S. H., Trudel, G. & Uhthoff, H. (2002) *Contemp. Top. Lab. Anim. Sci.* **41,** 21–26.
38. Sabatini, M., Boyce, B., Aufdemorte, T., Bonewald, L. & Mundy, G. R. (1988) *Proc. Natl. Acad. Sci. USA* **85,** 5235–5239.
39. Sato, K., Fujii, Y., Kasono, K., Ozawa, M., Imamura, H., Kanaji, Y., Kurosawa, H., Tsushima, T. & Shizume K. (1989) *Endocrinology* **124,** 2172–2178.
40. Manolagas, S. C. (2000) *Endocr. Rev.* **21,** 115–137.
41. Pacifici, R. (1996) *J. Bone Miner. Res.* **11,** 1043–1051.
42. Jimi, E., Nakamura, I., Duong, L. T., Ikebe, T., Takahashi, N., Rodan, G. A. & Suda, T. (1999) *Exp. Cell Res.* **247,** 84–93.
43. Li, H., Cuartas, E., Cui, W., Choi, Y., Crawford, T. D., Ke, H. Z., Kobayashi, K. S., Flavell, R. A. & Vignery, A. (2005) *J. Exp. Med.* **201,** 1169–1177.
44. Goldring, S. R. (2003) *Rheumatology* **42,** Suppl. 2, ii11–ii16.
45. Zalavras, C., Shah, S., Birnbaum, M. J. & Frenkel, B. (2003) *Crit. Rev. Eukaryot. Gene Expr.* **13,** 221–235.
46. Taishi, P., Chen, Z., Obal, F., Hansen, M., Zhang, J., Fang, J. & Krueger, J. (1998) *J. Interferon Cytokine Res.* **18,** 793–798.
47. Hunter, C. A., Jennings, F. W., Kennedy, P. G. & Murray, M. (1992) *Lab. Invest* **67,** 635–642.
48. Martin, T. J. (1993) *Osteoporos Int.* **3,** Suppl. 1, 121–125.
49. Nakamura, M., Udagawa, N., Matsuura, S., Mogi, M., Nakamura, H., Horiuchi, H., Saito, N., Hiraoka, B. Y., Kobayashi, Y., Takaoka, K., *et al.* (2003) *Endocrinology* **144,** 5441–5449.
50. Baldock, P. A., Sainsbury, A., Couzens, M., Enriquez, R. F., Thomas, G. P., Gardiner, E. M. & Herzog, H. (2002) *J. Clin. Invest.* **109,** 915–921.
51. Takeda, S., Elefteriou, F., Levasseur, R., Liu, X., Zhao, L., Parker, K. L., Armstrong, D., Ducy, P. & Karsenty, G. (2002) *Cell* **111,** 305–317.